

UC Irvine

UC Irvine Previously Published Works

Title

Magnetism in CePtPb

Permalink

<https://escholarship.org/uc/item/76t62789>

Journal

Physical Review B, 53(9)

ISSN

2469-9950

Authors

Movshovich, R
Lawrence, JM
Hundley, MF
[et al.](#)

Publication Date

1996-03-01

DOI

10.1103/physrevb.53.5465

Copyright Information

This work is made available under the terms of a Creative Commons Attribution License, available at <https://creativecommons.org/licenses/by/4.0/>

Peer reviewed

Magnetism in CePtPb

R. Movshovich, J. M. Lawrence,* M. F. Hundley, J. Neumeier, and J. D. Thompson
Los Alamos National Laboratory, Los Alamos, New Mexico 87545

A. Lacerda
National High Magnetic Field Laboratory, Los Alamos, New Mexico 87545

Z. Fisk
Florida State University, Tallahassee, Florida 32306
 (Received 14 June 1995; revised manuscript received 18 September 1995)

We report the behavior of the hexagonal compound CePtPb, which has an antiferromagnetic transition at $T_N=0.9$ K. The magnetic susceptibility is highly anisotropic, with the ratio χ_{ab}/χ_{ac} extrapolating to the value 65 at T_N . The low-temperature magnetization is also anisotropic with M_{ab} saturating to $0.92\mu_B/\text{Ce}$ atom at $B=5$ T, where M_c is five times smaller. The anisotropy is due both to low-symmetry crystal fields and to exchange anisotropy, which causes basal plane ferromagnetic fluctuations to develop below $T\approx 15$ K. Three facts suggest that the magnetic order might coexist with heavy-fermion behavior: heat-capacity data show a linear-in-temperature contribution $\gamma\approx 300$ mJ/mol K² in the antiferromagnetic state; the resistivity is quadratic in temperature below T_N ; and the magnetic entropy is generated very slowly with temperature reaching a value of only $0.7R \ln 2$ at $T=2T_N$. On the other hand, the long high-temperature tail of the heat-capacity data correlates with the ferromagnetic fluctuations above T_N ; and ac susceptibility measurements under hydrostatic pressure (to 17 kbar) show that T_N increases with pressure at an approximate rate 20 mK/kbar, which suggests that CePtPb sits in the small \mathcal{F} limit of the Doniach phase diagram; hence heavy-fermion effects may be negligible.

I. INTRODUCTION

In this paper we report experimental measurements of the susceptibility, magnetization, specific heat, and resistivity of single crystals of a new compound, CePtPb. This compound is related to a set of Ce ternary compounds which grow in the hexagonal Fe₂P structure, and which exhibit a spectrum of magnetic behavior,¹ from antiferromagnetic (CePdIn) to nonmagnetic heavy fermion (CePtIn) to mixed valent (Ce-NiIn). In the Fe₂P structure, the low site symmetry of the Ce ion (*mm*) should lead to anisotropy due to strong crystal-field effects. Since most experiments in these compounds have been done in polycrystals, where anisotropy cannot be observed directly, a major theme of this paper is to characterize the magnetic anisotropy in CePtPb. As we will show, the anisotropy arises both from crystal fields and from exchange anisotropy. A second major theme is whether the antiferromagnetic ordering which occurs in CePtPb at $T_N=0.9$ K coexists with heavy-fermion behavior. Such coexistence is expected when T_N is of the same order as the Kondo temperature T_K ; recent theory² suggests that such coexistence has profound consequences for the low-temperature behavior. Recently Beyermann *et al.*³ have argued that the compound CePt₂Sn₂ manifests such behavior. We discuss whether this occurs or whether more conventional magnetic order occurs in CePtPb.

II. EXPERIMENTAL DETAILS

Single crystals of CePtPb and LaPtPb of typical dimensions $2\times 2\times 10$ mm³ were precipitated from molten Pb;

most of the excess Pb was removed in a centrifuge. The crystals show a hexagonal habit, with the needle axis along the *c* axis. X-ray diffraction on powdered crystals yielded a hexagonal pattern with lattice constants $a_0=7.74$ Å, $c_0=4.13$ Å for CePtPb, and $a_0=7.77$ Å, $c_0=4.16$ Å for LaPtPb. The line intensities were in reasonable agreement with those expected for the ordered Fe₂P structure (*P62m*); but since the diffractometer (a Rigaku Miniflex) was not optimal for structural determination there remains uncertainty as to this assignment.

To establish reproducibility, all the following measurements were performed on at least two different samples, typically from different batches of crystal growth. Susceptibility measurements from 2 to 350 K were performed in a commercial SQUID magnetometer in fields of 0.1 T. Magnetization measurements were made with a vibrating sample magnetometer in an 18 T superconducting magnet at the National High Magnetic Field Laboratory, Pulsed Field Facility Los Alamos (NHMFL). Heat-capacity data were obtained using two experimental setups: relaxation calorimetry in a pumped helium station was used between 1.5 and 20 K, while a semiadiabatic heat-capacity cell in a dilution refrigerator was used between 80 mK and 1.7 K. Electrical resistance was measured on samples that were polished into rods with a rectangular cross section; this allowed easy determination of the geometrical factor for conversion of resistance into resistivity. Furthermore, the surfaces of unpolished crystals were covered with a thin layer of lead, which caused the resistance to vanish below the lead superconducting transition temperature ($T_c=7.19$ K); polishing removed the residual lead and allowed for measurements below that temperature. The resis-

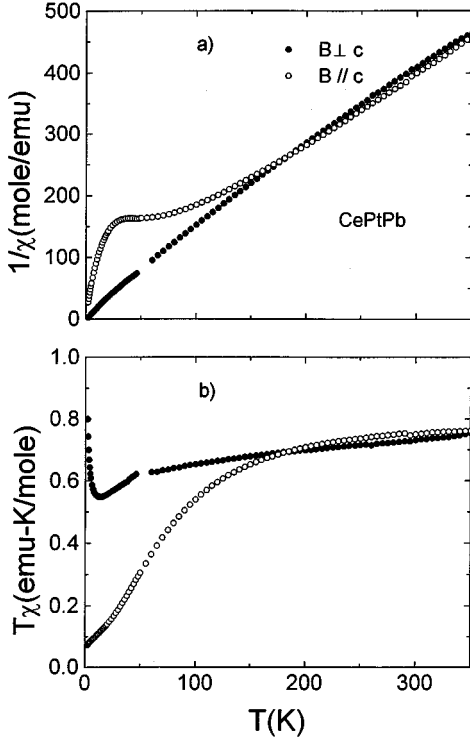


FIG. 1. Susceptibility of single-crystal CePtPb for the temperature range 2–350 K. Solid circles, χ_{ab} ; open circles, χ_c . The inverse of χ is plotted in (a), while the “effective moment” $T\chi$ is plotted in (b).

tivity data between room temperature and 1.2 K were collected in a pumped He apparatus; data between 40 mK and 1.6 K were collected in the dilution refrigerator station.

ac magnetic susceptibility measurements at ambient and hydrostatic pressure to 17 kbar took advantage of the fact that the susceptibility in the basal plane is strongly enhanced below 10 K due to ferromagnetic fluctuations (see below). A single-crystal rod of CePtPb was broken along the c axis into pieces of roughly similar sizes along all three dimensions, and the pieces were stacked together and glued with silver epoxy in such a way that they formed a rod with the axis now lying in the a - b plane of “easy” magnetization. The secondary coil was wound directly on the sample; the primary coil was wound on a brass former that slipped around the self-clamping Be-Cu pressure cell.⁴ A superconducting lead manometer was used to measure hydrostatic pressure in the cell.

III. RESULTS AND ANALYSIS

The inverse of the susceptibility for $2 < T < 350$ K and for fields of 0.1 T both parallel and perpendicular the c axis is shown in Fig. 1. For $T > 150$ K the susceptibilities χ_{ab} (for $B \perp c$) and χ_c (for $B // c$) are equal to within a few percent; the average value follows a Curie-Weiss law $\chi = C/(T + \Theta)$ with $C \approx 0.85$ emu/mol K (nearly equal the $J = 5/2$ free-ion value) and $\Theta \approx 40$ K. For temperatures below 150 K a strong anisotropy develops, with the easy axis being in the basal plane. The anisotropy ratio χ_{ab}/χ_c is 2 at 50 K and reaches 11 at 2 K. A plot of the “effective moment” $T\chi$ [Fig. 1(b)]

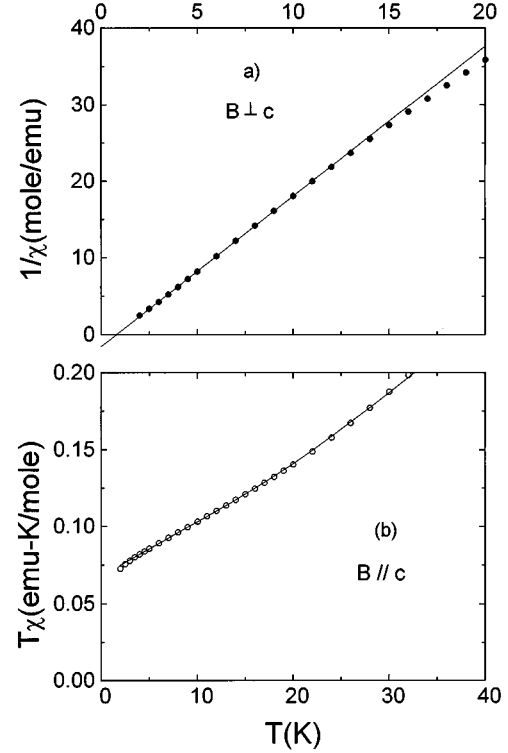


FIG. 2. Susceptibility of CePtPb at low temperature. (a) $1/\chi_{ab}$ vs temperature for $1.8 < T < 20$ K. The solid line represents $C_{ab}/(T - \Theta)$ with $C_{ab} = 0.51$ emu K/mol and $\Theta = 0.8$ K. (b) $T\chi_c$ vs T for $1.8 < T < 40$ K. The solid line represents the form $[\chi_{0,c} + (C_c/T) + (C_2/T) \exp(-\Delta/T)]/[1 + \exp(-\Delta/T)]$ with $\chi_{0,c} = 0.0035$ emu/mol, $C_c = 0.068$ emu K/mol, $C_2 = 0.58$ emu K/mol, and $\Delta = 100$ K.

shows that this anisotropy increases as the temperature is lowered.

The quantity $T\chi_c$ saturates to a value 0.068 emu K/mol at the lowest temperatures. A fit to the low-temperature behavior [Fig. 2(b)] shows that below 20 K χ_c varies as $\chi_{0,c} + (C_c/T)$ with $\chi_{0,c} = 0.0035$ emu/mol and $C_c = 0.068$ emu K/mol. Above 20 K, $T\chi_c$ increases more rapidly, due to the contribution of a higher-lying crystal-field state; the fit in Fig. 2(b) assumes a second doublet an energy 100 K above the ground state. The quantity $T\chi_{ab}$ has a minimum at 13 K and then increases dramatically at lower temperature [Fig. 1(b)]. The least-squares fits below 10 K show that χ_{ab} varies as $C_{ab}/(T - \Theta)$ where $C_{ab} = 0.51$ emu K/mol and $\Theta = 0.8$ K [Fig. 2(a)]. Extrapolating the fits for χ_{ab} and χ_c , we predict an anisotropy ratio $\chi_{ab}/\chi_c = 65$ at T_N .

The behavior of χ_{ab} suggests the approach to a ferromagnetic transition below 2 K. However, ac susceptibility measurements [Fig. 3(a)] show that the actual ground state is antiferromagnetic, with Néel temperature $T_N \approx 0.9$ K. Hence, the large magnitude of χ_{ac} represents ferromagnetic fluctuations with easy axis in the basal plane for $T > T_N$. In Fig. 3(b) we show further that the Néel temperature increases slowly with pressure, at the approximate rate 0.02 K/kbar.

In Fig. 4 we plot the magnetization in the range $0 < B < 18$ T at fixed temperatures of 2.3, 4, 20, and 100 K. The anisotropy is already visible at 100 K, and grows markedly stronger at low temperatures; at 2.3 K and 5 T it can be

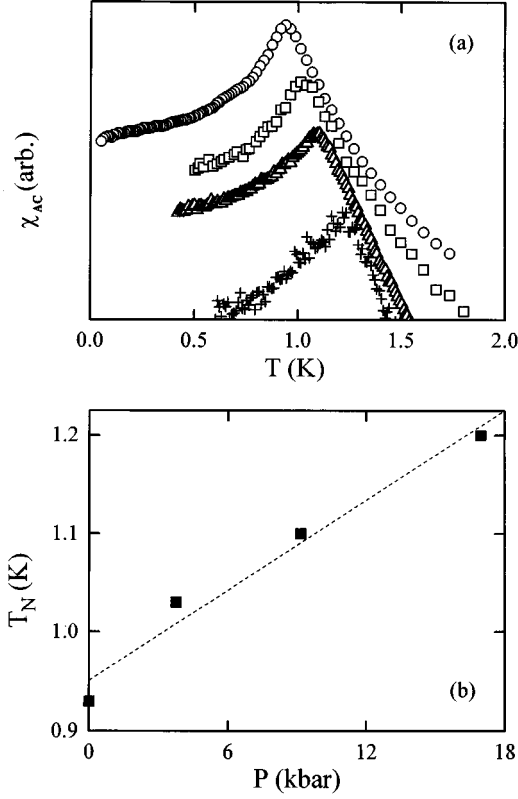


FIG. 3. (a) The ac susceptibility of CePtPb at low temperature and for several pressures for $B \perp c$. The units of χ_{ab} are arbitrary. (b) The Neel temperatures T_N (assuming the maximum in χ_{ab} occurs at T_N) plotted vs pressure.

seen that $M_{ab}/M_c = 5.5$. It can also be seen that at low temperature a field of order 10 T is sufficient to saturate M_{ab} while M_c continues to increase with field. The solid line in Fig. 4(a) represents the functional form

$$M_{ab} = (g_{ab}/2)\mu_B \tanh[g_{ab}\mu_B B/2k(T - \Theta)] + \chi_{0,ab}B. \quad (1)$$

The Brillouin term is that expected for a ground-state doublet (effective $S = 1/2$) with a spectroscopic g factor g_{ab} and with the ferromagnetic fluctuations treated in the mean-field approximation. The linear term $\chi_{0,ab} = 0.0065\mu_B/T = 0.0036$ emu/mol is the same as the constant term $\chi_{0,c}$ in the low-field c -axis susceptibility; the observed saturation magnetization is $M_{s,ab} = g_{ab}\mu_B/2 = 0.92\mu_B$ and the observed values for Θ are 1.3 K at 2.3 K and 1.8 K at 4 K. These values should be compared to the values $g_{ab/2} = 1.17$ and $\Theta = 0.8$ K obtained from the fits to the low-field, low-temperature susceptibility $\chi_{ab} = C_{ab}/(T - \Theta)$ assuming $C_{ab} = N_A(g_{ab}\mu_B)^2/4k_B$. At low fields the c -axis magnetization can be fit to a Brillouin (mean-field) term, with $M_{s,c} = 0.2\mu_B/\text{Ce atom}$ and $\Theta = 1.8$ K [Fig. 4(b), dashed line]; these values should be compared to the values $g_c/2 = 0.42$ and $\Theta = 0$ obtained from the fits to the low-field, low-temperature susceptibility $\chi_c = \chi_{0,c} + C_c/T$. Addition of the linear term $\chi_{0,c}B$ to this Brillouin term [Fig. 4(b), solid line] gives the right order of magnitude for M_c at 18 T, but makes it clear that to fit at higher fields requires an additional susceptibility which is nonlinear in B .

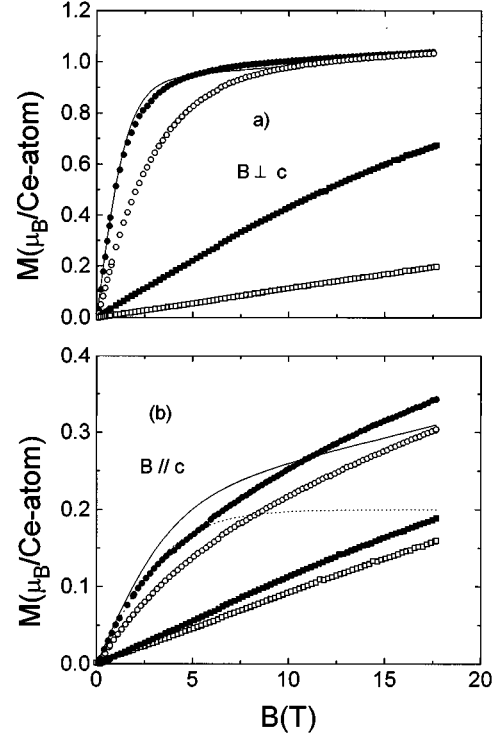


FIG. 4. The magnetization of CePtPb for fields $0 < B < 18$ T and at four temperatures: 2.3 K, solid circles; 4 K, open circles; 20 K, solid squares; and 100 K, open squares. M_{ab} is plotted in (a), and M_c is plotted in (b). The units are μ_B/atom ; the conversion factor to emu units is $1.791 \times 10^{-4} \mu_B/\text{atom} = 1$ emu/mol. The solid lines represent the sum of a Brillouin term and a linear term [Eq. (1); see text for details] while the dashed line represents a Brillouin term only.

The resistivity between 1.2 and 300 K is shown in Fig. 5(a). The overall behavior is that of a simple metal. The inset in Fig. 5(a) shows the region below 10 K; below 4 K the resistivity begins to decrease more rapidly with temperature. Figure 5(b) is a plot of the resistivity data between 40 mK and 1.6 K. The data show an upward kink upon cooling through the phase transition at $T_N = 0.9$ K. The inset of Fig. 5(b) shows that below 0.7 K the resistivity has a temperature dependence of the form $\rho = \rho_0 + AT^2$; a linear fit to the data gives $A = 0.24 \mu\Omega \text{ cm/K}^2$.

The specific heat of CePtPb and LaPtPb between 80 mK and 20 K is given in Fig. 6(a). The large peak at $T_N = 0.9$ K is expanded in the inset. Given that the lattice constants of the two compounds are nearly equal, we assume that the data for LaPtPb represent the phonon contribution to the specific heat of CePtPb, and that the $4f$ (magnetic) contribution to the specific heat of CePtPb can be taken as the difference $C_m(T) = C(\text{CePtPb}; T) - C(\text{LaPtPb}; T)$. The magnetic contribution $C_m(T)$ is plotted in Fig. 6(b). In Fig. 7(a) we plot the linear coefficient C_m/T ; this has a minimum at 0.030 J/mol K² near 12 K. For $T < T_N$, a plot of C/T vs T^2 [Fig. 7(a), inset] demonstrates that $C_m = \gamma(0)T + \beta(0)T^3$; least-squares fitting the data for the interval [0.2, 0.7 K] gives $\gamma(0) = 0.3$ J mol K² and $\beta(0) = 7.9$ J mol K⁴. We integrate C_m/T to obtain the magnetic entropy in Fig. 7(b). The increase above the value $R \ln 2$ for $T > 7$ K is expected due to the contribution of higher-lying crystal-field levels. In Fig.

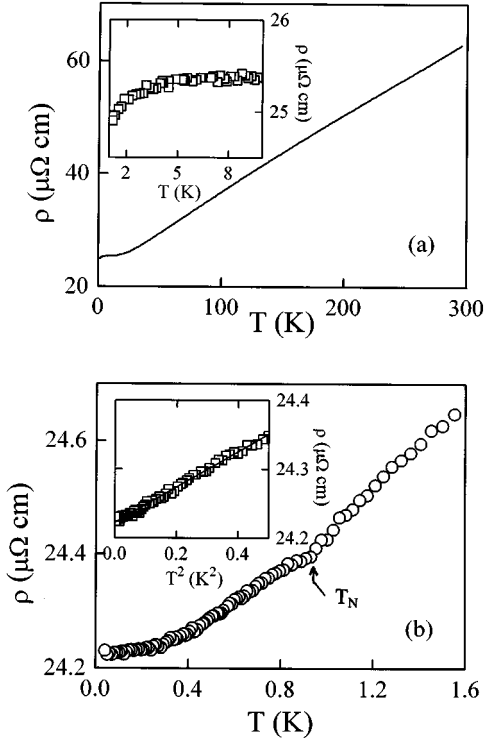


FIG. 5. (a) Resistivity of CePtPb between 1.2 and 300 K. Inset: Resistivity between 1.2 and 10 K. (b) Resistivity between 50 mK and 1.6 K. The upward kink at $T_N=0.9$ K suggests that the antiferromagnetism gaps the Fermi surface. Inset: resistivity plotted vs T^2 for $T < T_N$. The solid line is a fit to a linear form $\rho = \rho_0 + AT^2$ with $A = 0.24 \mu\Omega \text{ cm K}^2$. This Fermi-liquid behavior suggests that part of the Fermi surface is not gapped by the antiferromagnetism, so that heavy electron behavior persists below T_N .

6(b) we show the contribution expected from a doublet lying at $\delta=80, 100$, or 120 K; the value $\delta=100$ K seems appropriate. [This is the same value used to describe the increase in susceptibility in Fig. 2(b).] When the contribution of such a doublet is subtracted, we find that the tail of the specific heat extends to 15 K [Fig. 6(b), solid circles]. However, we obtain a slightly large value ($1.09R \ln 2$) for the saturation entropy in the ground-state doublet, suggesting that the analysis is incomplete (e.g., we need to include the third doublet expected for $J=5/2$ Ce).

IV. DISCUSSION

A. Anisotropy and crystal fields

Our x-ray-diffraction results show that CePtPb is hexagonal; the line intensities are in reasonable agreement with those expected for the Fe_2P structure, for which the Ce atom sits at the $3g$ site which has mm symmetry. For such a low-site symmetry, anisotropy of the susceptibility is expected on very general grounds.

Our measurements indeed show an anisotropy of the susceptibility developing below 150 K. The c -axis low-field susceptibility χ_c extrapolates at low temperature to a Curie constant $C_c = 0.068$ emu K/mol. Ignoring the low-temperature upturn [Fig. 1(b) in $T\chi_{ab}$] and extrapolating the data taken above 15 K to $T=0$ gives a low-temperature Cu-

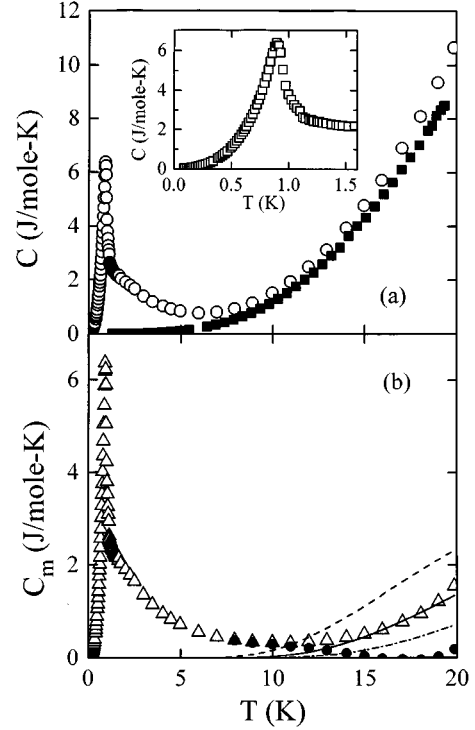


FIG. 6. (a) Heat capacity $C(T)$ of CePtPb and LaPtPb for $0.2 < T < 20$ K. Inset: $C(T)$ for CePtPb in the region of the antiferromagnetic transition, showing a peak at $T_N=0.9$ K. (b) The magnetic specific heat $C_m = C(\text{CePtPb}) - C(\text{LaPtPb})$. The lines show the expected contribution from a crystal-field doublet located at an energy $k_B\delta$ above the ground doublet. The value $\delta=100$ K gives the best representation of the data. The solid circles represent the magnetic specific heat after subtraction of the contribution of the higher doublet, with $\delta=100$ K. The contribution of the ground-state doublet is seen to be highly asymmetric above and below T_N , and to extend to very high temperatures (15 K) relative to T_N .

rie constant C_{ab} of order 0.5 emu K/mol. The low-temperature upturn, which arises from ferromagnetic exchange in the basal plane, can be fit in the Curie-Weiss approximation [Fig. 2(a)] where the resulting Curie constant is also 0.51 emu K/mol. The low-symmetry crystal field thus creates an easy plane and a susceptibility anisotropy $C_{ab}/C_c = 7.5$; the additional enhancement of the anisotropy for $T < 15$ K is an exchange effect. The existence of Van Vleck terms [i.e., the constant susceptibility $\chi_{0,c}$ at low temperature, Fig. 2(b)] is an additional typical consequence of low-symmetry crystal fields.

The saturation magnetization determined from the Brillouin fits to M_{ab} [Fig. 4(a)] implies a spectroscopic g factor $g_{ab}/2=0.92$, which is in qualitative agreement with the value 1.17 obtained from the low-temperature susceptibility. As mentioned in Sec. III, it is not possible to fit the low-temperature c -axis magnetization with the sum of a Brillouin term and a linear term over the entire range of field; although the fit works well at low field and gives the right order of magnitude for M_c at high field, it gives a very bad fit at intermediate fields [Fig. 4(b), dashed line]. Furthermore, there is a marked disagreement between the value $g_c/2=0.20$ obtained from this fit and that expected (0.425) on the basis of the extrapolated Curie constant.

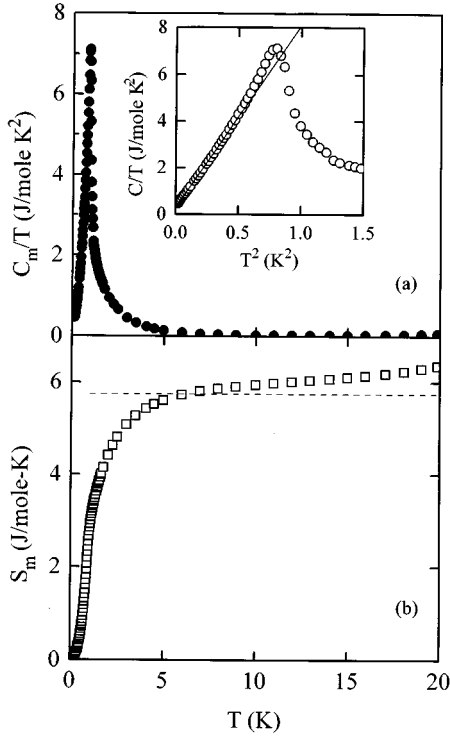


FIG. 7. The “linear coefficient” $C_m(T)/T$ plotted vs temperature. The inset details the region below T_N , plotting C_m vs T^2 . The solid line represents a fit to the form $\gamma(0)T + \beta(0)T^3$ with $\gamma(0) = 0.3 \text{ J/mol K}^2$. This large value is consistent with the value of the coefficient A [Fig. 5(b), inset] and supports the existence of heavy-fermion behavior below T_N . (b) The magnetic entropy S_m . The generation of entropy is very slow relative to T_N ; it is only $0.7R \ln 2$ at $2T_N$ and it recovers the full $R \ln 2$ entropy only at $7-8T_N$.

Clearly, the fits to $M(B)$ and to the low-field susceptibility χ are only qualitatively consistent; the quantitative discrepancies reflect the influence of higher-lying crystal-field doublets and require inclusion of nonlinear terms in the magnetization. Ignoring the effect of the highest-lying doublet, the increases in both χ_c and $C(T)$ above about 20 K [Figs. 2(b) and 6(b)] can be explained with a second doublet located 100 K above the ground-state doublet. The Curie constant for this doublet obtained from the fit in Fig. 2(b) would then be 0.58 emu K/mol , which implies a moment for the second doublet of order $1.2\mu_B/\text{atom}$ and hence a g factor of 2.4. In the large fields ($\sim 20 \text{ T}$) used in this experiment, this doublet could give rise to large nonlinear mixing into M_c . Consistent fits of the susceptibility, magnetization, and specific heat clearly require a much better knowledge of the actual crystal-field scheme, determined for example by inelastic neutron scattering, and a nonlinear calculation of the magnetization; this is beyond the scope of the present paper.

While the anisotropy of the saturation magnetization and of the susceptibility for $T > 15 \text{ K}$ can be explained as a crystal-field effect, the additional increase in $T\chi_{ab}$ below 15 K is clearly an exchange effect and can only arise from ferromagnetic fluctuations. All other mechanisms (crystal fields, heavy-fermion demagnetization, and antiferromagnetic fluctuations) cause $T\chi$ to decrease with decreasing temperature.

The existence of ferromagnetic fluctuations above the Néel temperature T_N of an antiferromagnet has been observed in other Ce compounds;⁵ it is expected when the exchange interaction J_{\parallel} between nearest Ce neighbors in the basal plane is ferromagnetic, but the interaction J_{\perp} between adjacent planes is antiferromagnetic. Nelson and Fisher⁶ have treated such a situation for Ising spins on a tetragonal lattice; in the mean-field regime, the ferromagnetic correlations tend towards a divergence at $\Theta = 2J_{\parallel} - J_{\perp}$ but the divergence is cut off by the antiferromagnetic transition, which in mean field occurs at $T_N = 2J_{\parallel} + J_{\perp}$. For the observed values $\Theta = 0.8 \text{ K}$ and $T_N = 0.9 \text{ K}$ this implies $J_{\parallel} = 0.425 \text{ K}$ and $J_{\perp} = 0.05 \text{ K}$ and an exchange anisotropy $J_{\perp}/J_{\parallel} = 0.12$. Of course, CePtPb is not tetragonal, and the spins are not Ising spins, so these estimates are merely qualitative. Exchange anisotropy and anisotropic order is very common in Ce compounds;⁵ it is believed to arise from hybridization of the localized f electron with the conduction electrons when the orbital character of the $4f$ wave function is correctly included.⁷

B. Coexistence of antiferromagnetism and heavy-fermion behavior

Doniach has proposed a phase diagram which is believed to be generic for heavy-fermion compounds.⁸ At small values of the Kondo coupling constant \mathcal{J} , magnetic order dominates and T_N increases as \mathcal{J}^2 ; for large \mathcal{J} Kondo demagnetization (with $T_K \propto \exp[-1/N(0)\mathcal{J}]$) dominates. At a critical value \mathcal{J}_c there is a $T=0$ transition from the antiferromagnetic ground state to a nonmagnetic Fermi liquid; at an intermediate value $\mathcal{J}_{\max} < \mathcal{J}_c$, there is a maximum in $T_N(\mathcal{J})$. The transition occurs when $T_N \approx T_K$, hence heavy-fermion behavior and magnetic correlations coexist for $\mathcal{J} \approx \mathcal{J}_c$; this leads to quantum critical behavior in the vicinity of the $T=0$ fixed point, which is expected to have profound consequences for the low-temperature behavior in both the magnetically ordered and the nonmagnetic regime.²

Recently Beyermann *et al.*³ have argued that the system CePt₂Sn₂, which undergoes antiferromagnetic ordering at $T_N = 0.9 \text{ K}$ is an example of the coexistence of magnetic order and heavy-fermion behavior. The argument was based on two features of the specific heat. The first is that the specific-heat coefficient $\gamma(T) = C(T)/T$ is very large (3.5 J/mol K^2) at temperatures just above T_N . The second is that on warming through T_N the spin entropy associated with the ordering ground-state doublet increases much more slowly than expected for a mean-field phase transition, reaching a value of only $0.7 R \ln 2$ as opposed to $R \ln 2$ at T_N . Both of these facts can be understood as consequences of heavy-fermion behavior. Using the Bethe-Ansatz result⁹ $T_K = \pi R/6\gamma$ where R is the gas constant gives $T_K = 1.2 \text{ K}$ for CePt₂Sn₂, which is of the same order as T_N . Furthermore, in the Kondo theory, the spin entropy is generated slowly (logarithmically) on the scale T/T_K , accounting for the slow growth of entropy above T_N .

Both these features are present in the data for CePtPb. In Fig. 6 it can be seen that the specific heat is highly asymmetric near T_N ; it decreases much more slowly for $T > 1.1 \text{ K}$ than in the comparable range for $T < T_N$. Above T_N the specific-heat anomaly appears to ride on a large background,

which increases slowly from 5 K to about 1.1 K, approaching a value of order 2 J/mol K at 1 K. If we interpret this weakly T -dependent asymmetric background as representing heavy-fermion behavior, with $\gamma(T_N) \approx 2$ J/mol K², we obtain $T_K \approx 2.2$ K, again of the same order as T_N . Second, as seen from Fig. 7(b), the entropy is generated even more slowly than in the case of CePt₂Sn₂, having the value $0.4R \ln 2$ at $T_N = 0.9$ K, the value $0.7R \ln 2$ at $T = 2T_N$ and reaching the full $R \ln 2$ expected for the doublet only at 7 K. Hence in this interpretation, the system demagnetizes and therefore loses spin entropy gradually as the temperature is lowered towards T_K ; but because $T_K \approx 2$ K is not much larger than $T_N \approx 1$ K, the demagnetization is insufficient to prevent magnetic order.

Other features of the data suggest that heavy-fermion behavior coexists with antiferromagnetism below T_N . The first is that the specific heat for $T < T_N$ behaves as $C(T) = \gamma(0)T + \beta(0)T^3$ [Fig. 7(a)]. The linear term [$\gamma(0) \approx 0.3$ J/mol K²] suggests that heavy-fermion behavior persists in the antiferromagnetic phase. Such linear behavior of $C(T)$ is also observed in U -based heavy-fermion antiferromagnets,¹⁰ supporting this interpretation. Second, the resistivity varies as AT^2 below T_N [Fig. 5(b), inset] with $A = 0.26 \mu\Omega \text{ cm}/\text{K}^2$. This power law, suggestive of Fermi-liquid behavior, is typically observed in nonmagnetic heavy-fermion compounds. Furthermore the ratio A/γ^2 has been found to have a typical value $1 \times 10^{-5} \mu\Omega \text{ cm}(\text{K mol/mJ})^2$ for heavy-fermion compounds;¹¹ for CePtPb the value of this ratio measured below T_N is $0.3 \times 10^{-5} \mu\Omega \text{ cm}(\text{K mol/mJ})^2$, which is within the range of variation expected for different compounds. Hence, there appears to be overall consistency with the view that heavy-fermion behavior persists in the ordered phase.

However, the argument is not conclusive. First of all, a slow generation of entropy, with $S(T_N) \sim 0.5R \ln 2$, is observed even for conventional antiferromagnets¹² due to fluctuations above T_N . Furthermore, the ferromagnetic correlations should contribute to the specific heat above T_N . After subtracting the estimated Schottky contribution from the higher doublet, the long high-temperature tail of the specific heat due to the ground-state doublet is observed [Fig. 6(b)] to persist out to the same temperature (about 15 K) as the ferromagnetic correlations. This suggests that the gradual loss of entropy below 15 K may be due to the onset of these correlations, rather than to the Kondo effect. (The situation is complicated even farther by the fact that magnetic correlations play an important role in establishing coherence, even in nonmagnetic heavy-fermion compounds.¹³)

A second caveat comes from the observation [Fig. 3(b)] that the Néel temperature increases with pressure. Since for Ce the application of pressure is expected¹⁰ to increase the hybridization responsible for the Kondo exchange (i.e., $d\mathcal{J}/dP > 0$), then in the context of the Doniach phase diagram we expect $dT_N/dP > 0$ when \mathcal{J} is smaller than the value where $T_N(\mathcal{J})$ is maximum. For small enough \mathcal{J} heavy-fermion effects should be negligible. As an example, we consider the study of CeT₂Si₂ compounds,¹⁴ where $T = \text{Ag, Au, Pd, Rh}$. All of these compounds order antiferromagnetically at a few tens of K. The hydrostatic pressure effects, however, differ dramatically across this row from

$dT_N/dP = +0.1$ and -0.04 K/kbar for $T = \text{Ag, Au}$, respectively, to -1.4 and -5 K/kbar for $T = \text{Pd, Rh}$, respectively. Coupled with other observations of the behavior of the resistance as a function of temperature and pressure, these results led to the conclusion that the Kondo temperature T_K was much lower than (CeAg₂Si₂) or comparable to (CeAu₂Si₂) the magnetic energy scale T_N , whereas the behavior of the other two compounds puts them in the opposite regime where $T_K > T_N$. This argument would lead to the conclusion that $T_N > T_K$ in CePtPb and that a much larger pressure is required¹⁵ to reverse the sign of dT_N/dP and to increase \mathcal{J} to a value sufficiently close to \mathcal{J}_c that heavy-fermion effects are non-negligible.

In this spirit, it is quite plausible that the linear coefficient of specific heat observed for $T < T_N$ (Fig. 7) and the T^2 dependence of the resistivity (Fig. 5) are artifacts of fitting the data over a limited temperature range, at insufficiently low temperature. We thus believe that the arguments given for the coexistence of ordering and heavy-fermion behavior are inconclusive for CePtPb [and quite possibly for CePt₂Sn₂ (Ref. 3) as well].

V. CONCLUSION

We have demonstrated that the susceptibility and magnetization of single crystals of the new compound CePtPb are highly anisotropic; and we have demonstrated that this anisotropy has its origin in the low-symmetry crystal field at the Ce site in the Fe₂P structure, with an additional enhancement due to exchange anisotropy, which causes ferromagnetic enhancement of the basal plane susceptibility at low temperatures. Given the large magnetic fields obtainable at NHMFL, nonlinear effects (beyond the Brillouin behavior of the ground-state doublet) need to be included in the calculation of the low-temperature magnetization. To obtain good fits between theory and measurement would require a better knowledge of the crystal-field splitting, best obtained from inelastic neutron scattering. A better determination of the crystal structure and cell parameters, by neutron or x-ray diffraction, is also in order.

The second issue raised by our work is whether heavy-fermion behavior coexists with antiferromagnetic order in CePtPb. The evidence for this comes from the linear behavior of the specific heat and the Fermi-liquid behavior ($\rho = AT^2$) of the resistivity for $T < T_N$, and from the large, slowly varying specific heat for $T > T_N$. On the other hand, the specific heat may be enhanced by ferromagnetic correlations rather than by Kondo demagnetization; and the observation that T_N increases with pressure suggests that CePtPb may be too far from the $T = 0$ magnetic-nonmagnetic transition for heavy-fermion effects to be important. Inelastic neutron scattering, which has recently been used¹³ to explore the coexistence of magnetic correlations in the ground state of nonmagnetic heavy-fermion compounds, is the ideal probe to resolve this issue.

ACKNOWLEDGMENTS

We thank Ward Beyermann and Paul Canfield for help at a preliminary stage of the experiment, George Kwei for cal-

culating the expected x-ray intensities, and Saul Oseroff and Andrew Millis for helpful discussions. Work at Los Alamos was performed under the auspices of the U.S. Department of Energy. The National High Magnetic Field Laboratory is

supported by the National Science Foundation. Work by J.M.L. was supported by the Center for Materials Science at Los Alamos under the auspices of the UC Personnel Assignment Program.

*Permanent address: Physics Department, University of California, Irvine, CA 92717.

¹K. Satoh, T. Fujita, Y. Maeno, Y. Uwatoka, and H. Fujii, *J. Phys. Soc. Jpn.* **59**, 692 (1990).

²U. Zülicke and A.J. Millis, *Phys. Rev. B* **51**, 8996 (1995).

³W.P. Beyermann, M.F. Hundley, P.C. Canfield, J.D. Thompson, Z. Fisk, J.L. Smith, M. Selsane, C. Godart, and M. Latroche, *Phys. Rev. Lett.* **66**, 3289 (1991).

⁴J.D. Thompson, *Rev. Sci. Instrum.* **55**, 231 (1984).

⁵J.M. Lawrence, K. Parvin, and S.M. Shapiro, *J. Phys. C* **19**, 2021 (1986).

⁶D.R. Nelson and M.E. Fisher, *Phys. Rev. B* **11**, 1030 (1975).

⁷Q.G. Sheng and B.C. Cooper, *Phys. Rev. B* **50**, 965 (1994).

⁸S. Doniach, in *Valence Instabilities and Related Narrow Band Phenomena*, edited by R.D. Parks (Plenum, New York, 1977), p. 169.

⁹V.T. Rajan, *Phys. Rev. Lett.* **51**, 308 (1983).

¹⁰J.D. Thompson and J.M. Lawrence, in *Handbook on the Physics and Chemistry of Rare Earths*, edited by K.A. Gschneidner, Jr., L. Eyring, G.H. Lander, and G.R. Choppin (Elsevier Science, British Vancouver, 1994), p. 383.

¹¹K. Kadowaki and S.B. Woods, *Solid State Commun.* **58**, 507 (1986).

¹²W.K. Robinson and S.A. Friedberg, *Phys. Rev.* **117**, 402 (1960).

¹³J. Rossat-Mignod, L.P. Regnault, J.L. Jacoud, C. Vettier, P. Lejay, J. Flouquet, E. Walker, D. Jaccard, and A. Amoto, *J. Magn. Magn. Mater.* **76&77**, 376 (1988).

¹⁴J.D. Thompson, R.D. Parks, and H. Borges, *J. Magn. Magn. Mater.* **54-57**, 377 (1986).

¹⁵A.L. Cornelius and J.S. Schilling, *Phys. Rev. B* **49**, 3955 (1994).